GEOPHYSICAL RESEARCH LETTERS, VOL. 27, NO. 19, PAGES 3117-3120, OCTOBER 1, 2000

Rotation and plate locking at the southern Cascadia subduction zone

Robert McCaffrey,[1] Maureen D. Long,[1] Chris Goldfinger,[2] Peter C. Zwick,[3]
John L. Nabelek,[2] Cheryl K. Johnson,[1] and Curt Smith[4]

Abstract. Global Positioning System vectors and surface tilt rates are inverted simultaneously for the rotation of western Oregon and plate locking on the southern Cascadia subduction thrust fault. Plate locking appears to be largely offshore, consistent with earlier studies, and is sufficient to allow occasional great earthquakes inferred from geology. Clockwise rotation of most of Oregon about a nearby pole is likely driven by collapse of the Basin and Range and results in shortening in NW Washington State. The rotation pole lies along the Olympic - Wallowa lineament and explains the predominance of extension south of the pole and contraction north of it.

1. Introduction

Oblique convergence of the young, oceanic Juan de Fuca plate with the western margin of North America (Fig. 1) results in both elastic deformation of coastal regions and distributed permanent deformation within the overriding plate. Evidence for large thrust earthquakes at the subduction zone is plentiful [*Adams*, 1990; *Atwater and Hemphill-Haley*, 1997; *Goldfinger et al.*, 1999] yet details of the earthquake history and potential are sketchy. Upper plate deformation, while clearly significant [*Pezzopane and Weldon*, 1993; *Wells et al.*, 1998], remains poorly quantified. We are using the Global Positioning System (GPS) to measure crustal deformation in western Oregon from which we infer strain rates in the overriding plate, the increase in the potential for earthquake slip on the Cascadia subduction fault, and how Oregon moves relative to North America.

2. Data and Analysis

We use horizontal vectors from 50 GPS sites in northwest Oregon analyzed by us, 21 published vectors from southern Oregon [*Savage et al.*, 2000] (Fig. 2), and four tilt rates near the Oregon coast [*Reilinger and Adams*, 1982]. We re-processed GPS campaign data collected by the US Geological Survey (1992-1994), by the Cascades Volcano Observatory (1992-1997), by us (1996-1999), and by a consortium of local observers under direction of the National Geodetic Survey (1998). Site positions were calculated in the ITRF96 reference frame [*Sillard et al.*, 1998] by combining campaign data with regional and global sites and precise satellite orbits using the GAMIT/GLOBK analysis software [*King and Bock*, 1999; *Herring*, 1998]. Site velocities and their covariances were estimated by linear regression of the time series of positions. Velocities were put in the North American (NA) reference frame by removing the NA-ITRF96 rotation [*DeMets and Dixon*, 1999], which agrees with our solution at the mm/a level for 16 NA sites. Convergence of the Juan de Fuca (JF) plate with NA is the sum of JF-Pacific [*Wilson*, 1993] and Pacific-NA [*DeMets and Dixon*, 1999] poles.

The 71 horizontal GPS vectors (2 components each) and 4 tilt rates provide 146 observations for the inversion. Misfit is defined by

$$\chi_n^2 = \frac{\Sigma_{i=1}^{N}(r_i/f\sigma_i)^2}{N-P} \quad (1)$$

where N is the number of observations, P is the number of free parameters, r_i is the residual (observed minus calculated velocity), σ_i is the formal velocity uncertainty, and f is a scaling factor. Formal GPS velocity uncertainties are well-known to be underestimated [*Mao et al.*, 1999] and $f = 3$ returns a minimum $\chi_n^2 \approx 1$. The final, unscaled standard deviations of residuals are 1.2 mm/a for the north component and 2.1 mm/a for the east. Velocity differences between our solution and *Savage et al.'s* [2000] were 1.2 and 1.3 mm/a for two common sites.

3. Inversion Approach

Our goal is to estimate the rotation of Oregon and plate locking on the Cascadia thrust from the geodetic data. Because plate locking strain extends hundreds of kilometers landward from the coast, the rotation pole and plate locking are estimated by a simultaneous inversion. Like many others, we describe plate locking as the fractional part (ϕ) of fault area that undergoes stick-slip and is currently stuck. The rate at which potential seismic moment (*i.e.*. moment that could later be released in earthquakes) builds is $\dot{M}_o = \phi\mu AV$ where A is fault area, V is the long-term slip rate on the fault, and μ is the shear modulus of rocks (40 GPa used here). Geodetic data constrain $\dot{M}_o$ because in an elastic medium surface deformation rates are proportional to ϕV.

To parameterize plate locking, we specify nodes every 10 km in depth and about every 100 km along strike on the thrust fault using the fault geometry of *Hyndman and Wang* [1995] (Fig. 3a). The convergence vector V_i at node i is calculated from the Juan de Fuca (JF) - western Oregon (WO) pole of rotation which is the sum of JF - North America (NA) and NA-WO poles. Plate locking, in the direction of JF-WO convergence, is $\phi_i V_i$. Interseismic surface deformation is estimated with an elastic, half-space dislocation model [*Okada*, 1985] by integrating over small, finite fault patches between nodes. ϕ at each patch is estimated by bilinear interpolation between the four enclosing nodes.

[1]Rensselaer Polytechnic Institute, Troy, New York
[2]Oregon State University, Corvallis, Oregon
[3]Seafloor Surveys International, Seattle, Washington
[4]National Geodetic Survey, Salem, Oregon

Paper number 2000GL011768.
0094-8276/00/2000GL011768$05.00

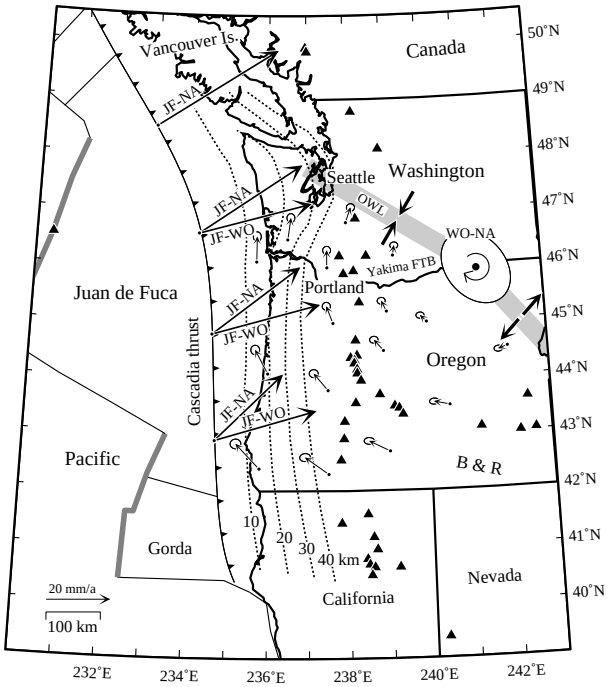

Figure 1. Pacific Northwest showing active volcanoes (triangles) and depth contours of the top of the subducting Juan de Fuca plate (dashed lines). Large arrows show convergence of Juan de Fuca plate with both North America (JF-NA) and the rotating Oregon block (JF-WO) at Cascadia deformation front. Ellipse in NE Oregon shows pole and 1σ uncertainty for rotation of WO relative to NA. Small arrows show velocities and 1σ uncertainties relative to NA predicted by this pole. Large opposing arrows show predicted sense of relative motion across the Olympic-Wallowa lineament (OWL).

We set $\phi = 0$ at the deepest nodes at 50 km depth, noting that interplate seismicity, and presumably locking, at most subduction zones ceases at about this depth [*Tichelaar and Ruff*, 1993]. To increase the sensitivity of the data for the estimated locking parameters, in some cases we grouped adjacent nodes into a single free parameter. For example, because land geodetic observations are insensitive to the near-trench locking, nodes at the trench were forced to have the same ϕ as adjacent nodes 10-km downdip. Model edges were handled by forcing nodes outside the GPS network to have the same coupling as adjacent nodes at the edge of the network. Other nodes were grouped if their uncertainties were large based on initial inversions in which all nodes were free and independent. To find parameter values that minimize misfit, we apply simulated annealing to downhill simplex minimization [*Press et al.*, 1989]. A penalty function keeps ϕ between 0 and 1 to prevent backslip or locking at a rate faster than plate convergence. At the minimum χ^2_n, we check for unconstrained parameters and calculate the covariance matrix with singular value decomposition of linearized normal equations.

We tested a range of models by varying the parameterization and constraints. With no motion of WO relative to NA and no plate coupling (no free parameters), minimum $\chi^2_n = 26.1$; when locking alone is allowed without rotation of Oregon (25 free parameters), $\chi^2_n = 7.2$; and rotation without plate locking (3 free parameters) gives $\chi^2_n = 2.5$. Hence, most of the data are explained by rotation of WO relative to NA. Our preferred model includes both coupling and rotation (Fig. 3) with 17 sets of free nodes, 3 pole parameters, and gives $\chi^2_n = 1.07$ (126 degrees of freedom). All four tilt rates are fit to within one standard error. Formal errors in all ϕ are less than 0.5.

4. Plate Locking

The final model suggests a double locked zone - one zone offshore and one near the down-dip edge of the fault at 30 to 40 km depth (Fig. 3a). We suspect that the inland locked zone might be an artifact for the following reason. Half-space dislocation models treat the base of the lithosphere effectively as a no-slip boundary in an elastic medium, resulting in unrealistically high resistance of the lithosphere to trench-normal contraction [*Thatcher and Rundle*, 1984] and a steep dropoff in surface velocities above the downdip edge of the coupled zone. Preliminary finite-element models in which low basal stress is allowed produce a gentler decay in velocities [*Williams and McCaffrey*, 1999] landward of the locked zone as seen in the data. Hence, we suggest that the majority of plate locking along the southern Cascadia subduction zone occurs offshore, in general agreement

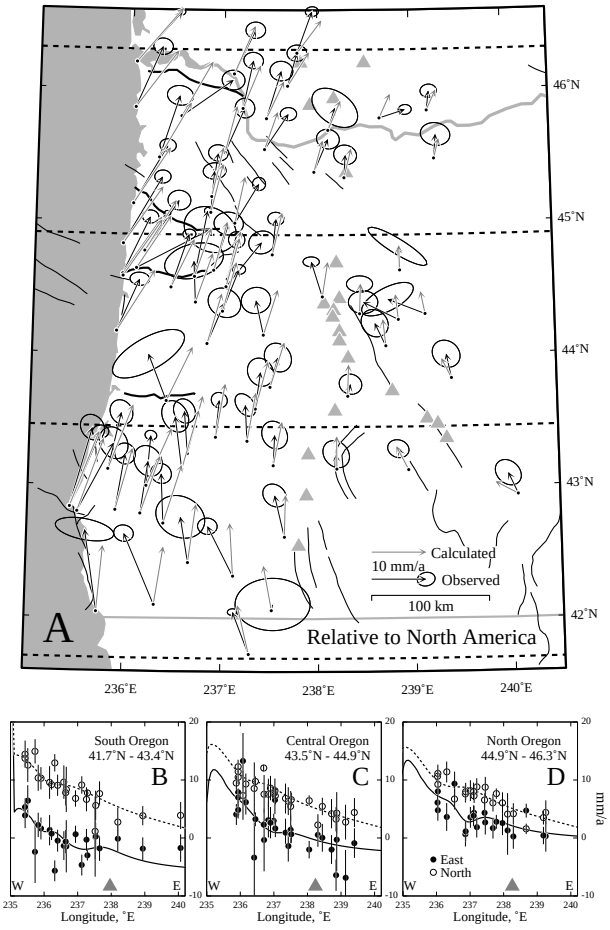

Figure 2. (a) Observed and calculated Oregon GPS site velocities relative to North America (NA) with 3σ ellipses. Black lines show locations of tilt lines. Dashed lines enclose profile regions. (b-d) West-to-East profiles of the North (open) and East (closed) components of the GPS vectors relative to NA (3σ error bars). Curves show predictions of rotation - locking model. Triangles show where profiles cross volcanic arc.

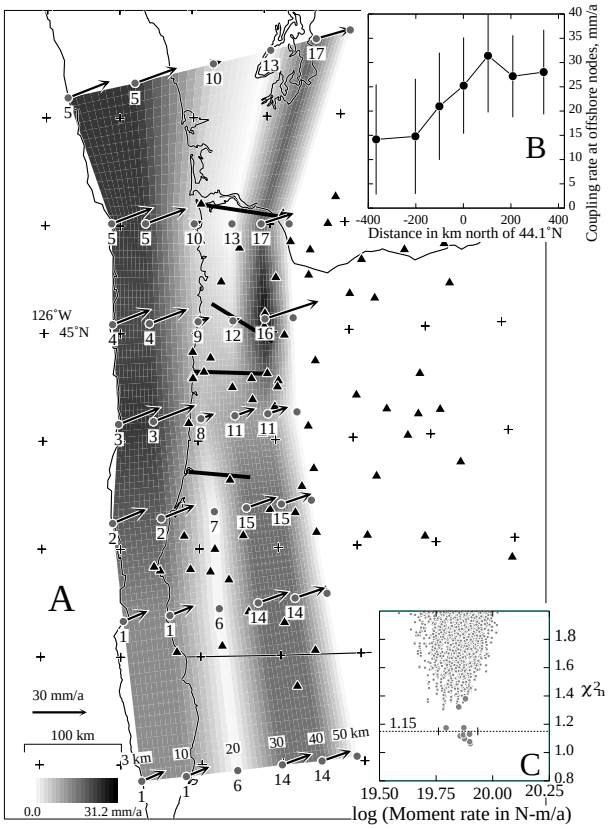

Figure 3. (a) Best-fit plate locking model. Gray dots show node locations on thrust fault. Nodes are aligned along depth contours - depths are given above southern set of nodes. Numbers below nodes are parameter indices, nodes sharing an index have same values of ϕ in inversion. Arrows show inferred locking rates at nodes. Darker shading indicates greater locking. Triangles show GPS sites and black bars show tilt lines. Tic spacing is 1°. (b) Variation in locking rates $\phi V(\pm\sigma)$along the margin at different depths. (c) Misfits for combinations of pole and node values and corresponding total geodetic moment rates. Large dots show best-fit solutions for various parameter sets; small dots are from grid searches. The uncertainty in moment rate, 10^{19} N-m/a, is the 99% confidence level, *i.e.,* an increase in χ^2_n of 0.08 ($\Delta\chi^2 = 9$ for 120 degrees of freedom) above the minimum χ^2_n =1.07 (shown by line at $\chi^2_n = 1.15$).

with inferences made from thermal and uplift data [*Hyndman and Wang*, 1995]. Coupling beneath land is possible but not required by the data. Because we had to smooth the model offshore, we cannot address whether the fault is locked out to the trench or not. Our results suggest a northward increase in the average offshore locking (Fig. 3b).

The geodetic moment rate estimated by integrating over the entire fault is $7\pm1 \times 10^{19}$ N-m/a (Fig. 3c), which is ~35% of full locking to 50 km depth. If this moment is released in earthquakes, in theory the earthquakes will be distributed as $N(M_o) = \alpha M_o^{-\beta}$ where N is the number of earthquakes of moment M_o or greater. The constant α depends on rates of earthquake activity, β governs the relative numbers of large and small quakes, and a maximum event size, M_o^{max}, is specified to keep the total moment finite. Dividing M_o^{max} by the total moment with $N(M_o^{max}) = 1$ shows that the ratio of the largest quake's moment to the total moment during the time T, the average repeat time of the largest earthquake [*Rundle*, 1989], is approximately 1-β [*McCaffrey*, 1997]. Hence, the total moment released during time T equals both $T\dot{M}_o$ (if $\dot{M}_o$ remains constant) and $M_o^{max}/(1-\beta)$, giving

$$T \approx \frac{M_o^{max}}{(1-\beta)\dot{M}_o}. \quad (2)$$

Great historic subduction earthquakes are thought to have occurred every 400 to 650 years, based on geologic evidence, along the southern 2/3 of the Cascadia thrust [*Adams*, 1990; *Atwater and Hemphill-Haley*, 1997]. The magnitudes of these events are not well-known, yet even if only $M_w \approx 9$ (*i.e.,* $M_o^{max} = 3.5 \times 10^{22}$ N-m and β=0) events occur and account for all the moment released, as thought by some [*Atwater and Hemphill-Haley*, 1997; *Goldfinger et al.*, 1999], the modern geodetic moment rate, if constant through time, is sufficient ($T = 500\pm70$ years).

Alternatively, at seismically active subduction zones β ranges from 0.56 to 0.80 [*Kagan*, 1997] and is in theory 2/3 [*Rundle*, 1989] meaning that earthquakes of various sizes release the moment. If southern Cascadia has a β value within this range and $M_w^{max} = 9$, the current moment rate is sufficient for a $M_w = 9$ approximately every 1000 to 2900 years, considering the range in β and $\dot{M}_o$. Also, during this time T there should be on average 7 to 16 $M_w \geq 8$ earthquakes, equivalent to one about every 150±30 years along the margin from 40°N to 46°N. If each of these earthquakes ruptures on average a 200-km segment of the 750-km long subduction zone, then each part of the fault will rupture every 550 years on average, also similar to the observed recurrence time. It should be noted that this latter view is inconsistent with recent interpretations by *Goldfinger et al.,* [1999] who imply a one-to-one correspondence between turbidites, that occur every 655 years, and $M_w = 9$ subduction zone earthquakes. While our geodetic data do not constrain past or future earthquake size distributions for Cascadia, the modern surface strain rate implies a rate of moment accumulation (as interpreted with a dislocation model) that is sufficient for either scenario.

5. Rotation of Oregon

The best-fit pole of rotation for WO-NA (at 45.9° ± 0.6°N, 241.3° ± 0.7 °E, with a clockwise rotation rate of 1.05 ± 0.16°/Ma, Fig. 1) is close to a pole inferred from geology [*Wells et al.*, 1998] but far from one estimated from southern Oregon GPS data [*Savage et al.*, 2000]. The eastward decrease in the northward motion of Oregon (Figs. 2b-d) is matched sufficiently by rotation about a pole to the east and does not require slip on faults in eastern Oregon. Nevertheless, slip may occur at the few mm/a level - below the uncertainties in the GPS measurements - as indicated by paleoseismology [*Pezzopane and Weldon*, 1993].

The WO-NA pole lies along the Olympic - Wallowa lineament (OWL) (Fig. 1) at the northern edge of the Basin and Range extensional regime and the southeastern edge of the Yakima fold-thrust belt [*Wells et al.*, 1998]. *Pezzopane and Weldon* [1993] show largely extensional structures along the OWL in Oregon and contractional structures along it in Washington, consistent with our pole location and clockwise rotation. Similarity of GPS vectors in SW Washington [*Khazaradze et al.*, 1999] to those in NW Oregon suggests that it rotates with Oregon (Fig. 1). The southern edge of

the WO block is likely in N. California but our data do not cover it.

Lack of an offset in the GPS north components at the volcanic arc (Fig. 2b-d) shows that it does not act as a block boundary, suggesting the north-moving Sierra Block at the south edge of the Oregon forearc is not driving the block rotation. If it is, eastern Oregon lithosphere (including the magmatic arc) would have to be very strong under tension to move coherently under a northwestward push at its SW corner. For the same reason, coast-parallel traction associated with oblique subduction of the Juan de Fuca plate under the forearc is probably not alone driving the block rotation. Oregon's sense of rotation and its lack of rapid internal deformation support the suggestion by *Humphreys and Hemphill-Haley* [1996] that it is moving in response to Basin and Range extension to the southeast. However, in contrast to their idea that the NW-directed extension of the Basin and Range is a response to a weak Cascadia subduction zone that allows westward escape of Oregon, the nearby pole of rotation ultimately results in N-S shortening in Washington or Canada and little change in the overall subduction rate at the Cascadia thrust. That Oregon rotates about a nearby pole suggests that the force resisting shortening at the subduction zone is sufficient to deflect Oregon's motion northward where it is instead accommodated by shortening in the continental lithosphere.

6. Conclusions

Inversion of GPS and tilt data from western Oregon reveal a clockwise rotation of Oregon relative to North America about a nearby pole superimposed on ENE-directed contraction arising from locking with the subducting Juan de Fuca plate. Geodetic estimates of rotation and locking are similar to those made from geologic, paleomagnetic, thermal, and uplift data. The extent of the Oregon block and its sense of rotation suggest that it is driven by Basin and Range extension and not by localized forces along its western edge. The NE boundary of the Oregon block, including SW Washington, appears to be along the Olympic - Wallowa lineament.

Acknowledgments. B. Atwater, C. Williams, R. Wells, and two GRL reviewers made useful comments. C. Stevens, R. King, T. Herring, and M. Murray advised on data processing. Many people assisted in field measurements. The U. S. Geological Survey and Cascades Volcano Observatory provided GPS data. Supported by National Science Foundation grant EAR-9814926 and by US Geological Survey under award 99HQGR0014. The views and conclusions contained in this document are those of the authors and should not be interpreted as official policies of the US Government. GPS velocities used in this paper are available at www.rpi.edu/∼mccafr/gps/grl00_or.dat.

References

Adams, J., Paleoseismicity of the Cascadia subduction zone: Evidence from turbidites off the Oregon-Washington margin, *Tectonics 9,* 569-583, 1990.

Atwater, B. F., and E. Hemphill-Haley, Recurrence intervals for great earthquakesof the past 3,500 years at northeastern Willapa Bay, Washington, *USGS Professional Paper 1576,* 1997.

DeMets, C. and T. H. Dixon, New kinematic models for Pacific-North America motion from 3 Ma to present, I: Evidence for steady motion and biases in the NUVEL-1A model, *Geophys. Res. Lett., 26,* 1921-1924, 1999.

Goldfinger, C., H. Nelson, and J. E. Johnson, Holocene recurrence of Cascadia great earthquakes based on the turbidite event record, *Eos Trans. AGU, 80,* F1024, 1999.

Herring, T. A., GLOBK: Global Kalman filter VLBI and GPS analysis program, v.4.1, Massachusetts Institute of Technology, Cambridge, 1998.

Humphreys, E., and M. A. Hemphill-Haley, Causes and characteristics of Western U.S. deformation, *Geol. Soc. Am. Abstracts, 28,* 1996.

Hyndman, R. D., and K. Wang, The rupture zone of Cascadia great earthquakes from current deformation and the thermal regime, *J. Geophys. Res., 100,* 22133-22154, 1995.

Kagan, Y. Y., Seismic moment-frequency relation for shallow earthquakes: Regional comparison, *J. Geophys. Res., 102,* 2835-2852, 1997.

Khazaradze, G., A. Qamar, and H. Dragert, Tectonic deformation in western Washington from continuous GPS measurements, *Geophys. Res. Lett., 26,* 3153-3156, 1999.

King, R. W. and Y. Bock, Documentation for the GAMIT GPS analysis software, Release 9.82, Massachusetts Institute of Technology, Cambridge, 1999.

Mao, A., C. G. A. Harrison, and T. H. Dixon, Noise in GPS coordinate time series, *J. Geophys. Res., 104,* 2797-2816, 1999.

McCaffrey, R., Statistical significance of the seismic coupling coefficient, *Bull. Seismol. Soc. Am., 87,* 1069-1073, 1997.

Okada, Y., Surface deformation due to shear and tensile faults in a half-space, *Bull. Seismol. Soc. Am., 75,* 1135-1154, 1985.

Pezzopane, S. K., and R. Weldon, Tectonic role of active faulting in central Oregon, *Tectonics, 12,* 1140-1169, 1993.

Press, W. H., B. P. Flannery, S. A. Teukolsky, and W. T. Vetterling, *Numerical Recipes,* Cambridge Univ. Press, Cambridge, 1989.

Reilinger, R., and J. Adams, Geodetic evidence for active landward tilting of the Oregon and Washington coastal areas, *Geophys. Res. Lett., 9,* 401-403, 1982.

Rundle, J., Derivation of the complete Gutenberg-Richter magnitude-frequency relation using the principle of scale invariance, *J. Geophys. Res., 94,* 12337-12342, 1989.

Savage, J. C., J. L. Svarc, W. H. Prescott, and M. H. Murray, Deformation across the forearc of the Cascadia subduction zone at Cape Blanco, Oregon, *J. Geophys. Res., 105,* 3095-3102, 2000.

Sillard, P., Z. Altamimi, and C. Boucher, The ITRF96 realization and its associated velocity field, *Geophys. Res. Lett., 25,* 3223-3226, 1998.

Thatcher, W., and Rundle, J. B., A viscoelastic coupling model for cyclic deformation due to periodically repeated earthquakes at subduction zones, *J. Geophys. Res., 89,* 7631-7640, 1984.

Tichelaar, B. W., and L. J. Ruff, Depth of seismic coupling along subduction zones, *J. Geophys. Res., 98*, 2017-2037, 1993.

Wells, R. E., C. S. Weaver, and R. J. Blakely, Forearc migration in Cascadia and its neotectonic significance, *Geology 26,* 759-762, 1998.

Williams, C. A., and R. McCaffrey, Modeling of surface deformation at subduction zones: alternatives to dislocation models, *Eos Trans. AGU, 80,* F266, 1999.

Wilson, D. S., Confidence intervals for motion and deformation of the Juan de Fuca plate, *J. Geophys. Res., 98,* 16,053-16,071, 1993.

C. Johnson, M. Long, and R. McCaffrey, Department of Earth and Environmental Sciences, Rensselaer Polytechnic Institute, Troy, NY 12180. (e-mail: mccafr@rpi.edu)

C. Goldfinger and J. Nabelek, College of Oceanic and Atmospheric Sciences, Oregon State University, Corvallis, OR 97330.

C. Smith, National Geodetic Survey, P.O. Box 12114, Salem, OR 97309.

P. Zwick, Seafloor Surveys International, 2727 Alaskan Way, Pier 69, Seattle, WA 98121.

(Received May 10, 2000; revised July 14, 2000;
accepted July 21, 2000.)